MODELLING OF SHORTWAVE RADIATION FOR SNOW COVERED TERRAIN

Stuart E. Waterman

Hydrometeorology Division
Atmospheric Environment Service
Downsview, Ontario

ABSTRACT

A solar radiation model is described which is capable of calculating the spectral distribution of the direct and diffuse components of the solar radiation incident upon a snow covered surface in clear-sky conditions. The model accounts for upwelling radiation backscattered toward the earth's surface, radiation reflected to a point from the surrounding terrain, and the anisotropy of the diffuse flux. Input of the spectral reflectance characteristics of the terrain allows calculation of the shortwave radiation absorbed by the snow surface. The accuracy of the model is assessed by comparison with available data.

Calculation of the net shortwave radiation received by inclined snow surfaces demonstrates the importance of terrain reflection and atmospheric backscattering in the shortwave radiation balance of snow covered terrain. These calculations further demonstrate that the majority of the solar radiation absorbed by snow surfaces is in the near infrared region of the spectrum. The results of the investigation suggest that it may be possible to omit the diffuse flux in calculations of net solar radiation over large areas of extensive snow cover.

INTRODUCTION

Solar radiation is recognized as a critically important component of the energy balance of a snowpack. In mountainous drainage basins solar radiation measurements are typically unavailable, and the components of the shortwave radiation balance must be obtained by empirical or analytical methods (e.g. Garnier and Ohmura, 1968, 1970, Williams et al, 1972). Wavelength integrated values of the shortwave flux are commonly used in such calculations for reasons of computational simplicity. However, recent studies by Dozier (1978), and Choudhury and Kukla (1979) have illustrated the importance of the spectral characteristics of the interaction between the incident solar flux and a snow surface. This paper describes a solar radiation model which is capable of calculating the spectral distribution of the various components of the shortwave radiation balance for snow covered terrain. The model is used to demonstrate the importance of spectral characteristics in calculations of the shortwave energy absorbed by snow surfaces in various topographic situations.

THE SOLAR RADIATION MODEL

Calculation of the components of the net solar radiation for a snow surface involves:

a) Calculation of the incident spectral irradiance for given atmospheric and topographic boundary conditions, including upwelling radiation backscattered toward the surface and radiation reflected from other terrain surfaces.

b) Calculation of the absorbed spectral flux, given the spectral reflectance characteristics of the snowpack. Integration of the net radiation distribution yields the total shortwave energy absorbed by the snow surface.

The solar radiation model used in this investigation is described in detail elsewhere (Waterman, 1980a,b). Therefore, the following description is intentionally brief, stressing those aspects of particular importance in calculations of net solar radiation for inclined snow surfaces, specifically the anisotropy of the diffuse spectral irradiance, atmospheric backscattering of upwelling radiation, and reflection of radiation directly to a surface from other terrain surfaces. The latter two factors, although often neglected in radiation modelling, can be critically important in the case of snow covered terrain of high albedo.

The model atmosphere is assumed to be cloudless, plane parallel and horizontally homogeneous. Vertical variations in atmospheric composition are described by simple analytical functions. Atmospheric scattering is confined to a single layer in the atmosphere. Atmospheric input parameters required by the model are either easily measured or readily available in the literature. The area of the earth's surface which yields the initial upwelling flux for subsequent backscattering is assumed to be horizontal and homogeneous. The spectral reflectance characteristics of all terrain surfaces in the model are specified as input. All surfaces are assumed to be Lambertian reflectors.

The solar spectrum from 0.285 to 3.0 μm is divided into 136 irregular intervals corresponding to the tabulations of the extraterrestrial flux given by Thekaekara (1973), which forms the basic input for the model. Within each spectral interval, the solar flux is assumed to be monochromatic and the optical properties of the atmosphere are assumed to be constant. Spectral integration of the flux density distributions is accomplished by the trapezoidal method.

For a given wavelength λ, the instantaneous value of the normal incidence direct beam irradiance is:

$$I_\lambda = I_{o\lambda} r^{-2} Tr_\lambda Ta_\lambda Tg_\lambda Tw_\lambda Toz_\lambda \qquad (1)$$

The atmospheric transmission functions for Rayleigh scattering, and absorption by water vapour, uniformly mixed gases, and ozone are calculated by the method of Leckner (1978), with slight modifications to the calculations of optical path length as described by Waterman (1980a). Aerosol attenuation is calculated by the method of Angstrom (1961, 1964), assuming that aerosol absorption is negligible. The radius vector of the earth's orbit, r, is calculated using the formula of Williams et al (1972). For illustrative purposes, it is sufficient to limit discussion to instantaneous values of the solar flux, although temporal integration can be easily performed by conventional methods (e.g. Robinson, 1966, Garnier and Ohmura, 1968, 1970, and Williams et al, 1972).

The direct beam irradiance received by a surface is:

$$S\downarrow_\lambda = I_\lambda \cos i \qquad (2)$$

where i is the angle of incidence of the solar beam, calculated by the method of Robinson (1966, p.41).

The remainder of the total irradiance received by the surface is in the form of a diffuse radiation flux, $D\downarrow_\lambda$, which has three components in the model: 1) scattered downwelling radiation, $D\downarrow s_\lambda$, 2) backscattered upwelling radiation, $D\downarrow b_\lambda$, and 3) radiation reflected directly to the surface from other terrain surfaces, $D\downarrow r_\lambda$.

Following the method proposed by Houghton (1954), and successfully applied by a number of subsequent investigators, including Temps and Coulson (1977) and Leckner (1978), the total amount of radiation scattered out of the incoming direct beam is given by

$$\Delta Is_\lambda = I_{o\lambda} r^{-2} Toz_\lambda Tg_\lambda Tw_\lambda (1 - Tr_\lambda Ta_\lambda) \qquad (3)$$

an adaption of equation 1 which yields the difference between the normal incidence direct irradiance, and a fictitious direct beam subject only to absorption. The combined effects of Rayleigh and Mie (aerosol) scattering cause the scattered radiation to be anisotropically distributed, a phenomenon which is difficult to evaluate analytically. The

model employs a simple parameterization of the anisotropic distribution which reproduces the most important spectral and geometric characteristics of the diffuse flux for the present application, specifically the dominance of forward scattering and the concentration of the downwelling diffuse flux in the circumsolar region of the sky hemisphere. The monochromatic diffuse radiation directed towards the earth's surface from the scattering layer is thus defined as:

$$Df_\lambda = f_\lambda \Delta Is_\lambda \tag{4}$$

The forward scattering factor, f_λ, is assumed to have a minimum value of 0.5 at all wavelengths, representing isotropic Rayleigh scattering in the absence of aerosols. In the presence of non-absorbing aerosols, which are here assumed to scatter in the forward direction only, f_λ is given by

$$f_\lambda = 1 - 0.5 \left(\frac{(1 - Tr_\lambda)}{(1 - Tr_\lambda Ta_\lambda)}\right)^{0.07} \tag{5}$$

(Waterman, 1980a).

The distribution of the downwelling diffuse flux within the sky hemisphere is characterized by a maximum in the zone surrounding the sun caused by small-angle aerosol scattering. For given atmospheric conditions, the anisotropy of the angular distribution increases with wavelength as a consequence of the increasing dominance of aerosol scattering at long wavelengths. Although this phenomenon is relatively unimportant in calculations of the diffuse irradiance for a horizontal surface, it may be a significant factor in more complex terrain situations. Following the method of Paltridge and Platt (1976, p.124) and Hay (1978a), the angular distribution of the downward scattered diffuse flux is modelled in the form of two discrete components: a circumsolar component, D↓cs, which is assumed to be coincident with the direct solar beam, and an isotropic component, D↓i. The fraction of the downwelling diffuse flux which is isotropically distributed is given by

$$fi_\lambda = 1 - (2f_\lambda - 1)^{0.3} \tag{6}$$

(Waterman, 1980a). The spectral distributions of f_λ and fi_λ for a typical model atmosphere are shown in figure 1.

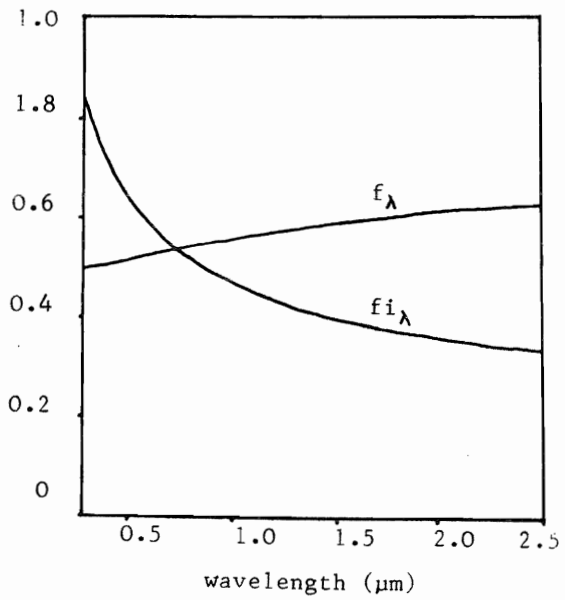

Figure 1. Typical spectral distributions of f_λ and fi_λ .

The isotropic component of $D\downarrow s_\lambda$ received by a sloping surface of inclination γ facing an infinite horizontal surface is, therefore:

$$D\downarrow i_\lambda = fi_\lambda \, Df_\lambda \cos z \cos^2(\gamma/2) \tag{7}$$

where z is the factor $\cos^2(\gamma/2)$ represents the fraction of the sky hemisphere exposed to the inclined surface. The circumsolar diffuse flux incident on the surface is

$$D\downarrow cs_\lambda = (1 - fi_\lambda) Df_\lambda \cos i \tag{8}$$

and $D\downarrow s_\lambda$ is, therefore

$$D\downarrow s_\lambda = Df_\lambda (fi_\lambda \cos z \cos^2(\gamma/2) + (1 - fi_\lambda) \cos i) \tag{9}$$

The backscattering of upwelling radiation is typically ignored in most radiation modelling investigations. However, the high reflectance of snow in the visible wavelengths suggests that this factor should be included in models for snow covered terrain. In the model, the backscattered component of the total diffuse irradiance, $D\downarrow b_\lambda$, is calculated by the method suggested by Obled and Harder (1978), which accounts for multiple reflection between the surface and the atmosphere. In this method the atmosphere is represented by a horizontal surface with an effective spectral reflectance pa_λ . If aerosol scattering is presumed to be confined to the forward direction, then backscattering is solely the result of isotropic Rayleigh scattering, and pa_λ is given by

$$pa_\lambda = 0.5 \, (1 - Tr_\lambda) \tag{10}$$

(Waterman, 1980a), where Tr_λ is calculated for a weighted average air mass of 1.66. The earth's surface contributing to the upwelling flux backscattered to the point in question is represented by a hypothetical sunlit horizontal surface of reflectance ps_λ. In order to account for the observed increase in surface reflectance at large solar incidence angles, the spectral reflectance of the horizontal surface is modified to account for Fresnel effects by the method suggested by Paltridge and Platt (1976, p.133), such that

$$ps_\lambda(z) = ps_\lambda + (1 - ps_\lambda)\exp(-0.1(90 - z)) \tag{11}$$

where $ps_\lambda(z)$ is the spectral reflectance of a horizontal surface at a given solar zenith angle and ps_λ is the spectral reflectance of the surface material for near normal incidence irradiance. Assuming that atmospheric absorption of the multiple reflected radiation is negligible, $D\downarrow b_\lambda$ is given by

$$D\downarrow b_\lambda = (D\downarrow s_\lambda + I_\lambda \cos z)(ps_\lambda(z) pa_\lambda / (1 - ps_\lambda(z) pa_\lambda)) \tag{12}$$

where $D\downarrow s_\lambda$ is calculated for a horizontal surface. The backscattered diffuse flux incident on a slope of angle γ is reduced by the factor $\cos^2(\gamma/2)$, as in equation 7.

Radiation reflected to a surface from other terrain surfaces can be a significant energy source in mountainous terrain, particularly in the presence of snow cover. For the purpose of the present discussion, a simple terrain model is used in which an inclined receiving surface is assumed to be essentially dimensionless and surrounded by an infinite horizontal surface. This model, although simplistic, has the advantage of accurately simulating the situation of an inclined radiometer suspended over a horizontal plane, thus facilitating verification of the model with easily obtained field measurements. The model is also a reasonable approximation to the situation of a long, straight inclined surface contiguous with a horizontal surface in those instances where the slope does not significantly shade the horizontal surface (i.e. where $\cos i \geq 0$). A version of the radiation model which deals with more realistic terrain configurations is described by Waterman (1980a,b). For the simple model, the sections of the hemisphere above an inclined surface which are subtended by the sky and by the horizontal plane are defined by the factors $\cos^2(\gamma/2)$ and $1 - \cos^2(\gamma/2)$, respectively. Thus, the reflected component of the diffuse flux received by the inclined surface is given by

$$D\downarrow r_\lambda = K\downarrow_\lambda h \, ps_\lambda(z)(1 - \cos^2(\gamma/2)) \tag{13}$$

where $K\downarrow_\lambda h$ is the total spectral irradiance incident on the horizontal surface.

The total irradiance received by the inclined surface is given by:

$$K\downarrow_\lambda = S\downarrow_\lambda + D\downarrow b_\lambda + D\downarrow s_\lambda + D\downarrow r_\lambda \quad (14)$$

If the reflectance of the surface is p_λ, then the reflected flux is

$$K\uparrow_\lambda = p_\lambda K\downarrow_\lambda \quad (15)$$

and the net solar flux K^*_λ is now defined.

MODEL PERFORMANCE

The calibration and verification of the model is discussed in detail elsewhere (Waterman, 1980a), and need not be repeated here. However, the performance of the model for the situation of an inclined surface facing a horizontal snow surface is of particular interest in this context. This was determined using hourly broad band irradiance data measured by the Atmospheric Environment Service of Canada (Hay, 1978b). These data include: normal incidence direct beam irradiance, I, total irradiance on a horizontal sensor, $K\downarrow h$, the reflected flux from the horizontal surface, $K\uparrow h$, and the total irradiance on south-facing sensors inclined at angles of 30, 60, and 90 degrees. The data available were collected over two winter seasons, from which 14 days have been selected as representing clear sky conditions in the presence of snow cover, the latter condition defined by a measured albedo in excess of 70 percent. Average hourly values for the period between 1100 and 1300 hours local apparent time were converted to an average instantaneous value for the two hour period. Ozone content and precipitable water values are estimated from the monthly average data published by Robinson (1966, p.114) and Hay (1971), respectively. In the absence of contemporaneous spectral reflectance measurements, the snow surface reflectance characteristics required to calculate $D\downarrow b_\lambda$ and $D\downarrow r_\lambda$ were estimated using the laboratory data of O'Brien and Munis (1975). The reflectance data used are shown in figure 2, and represent two dissimilar snow conditions: 1) fresh snow of low desnity and high wavelength - integrated reflectance (approximately 0.84), and 2) older snow of higher density and lower reflectance (approximately 0.74).

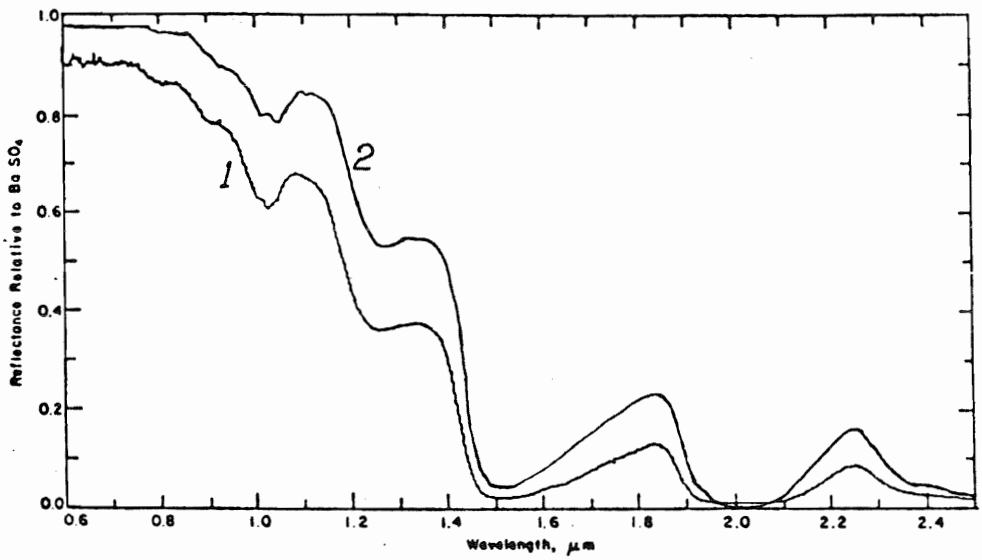

Figure 2. Spectral reflectance distributions used to calculate irradiance at the Toronto measurement site.

The spectral reflectance curve input to the model for a given date was the one whose integrated reflectance was closest to the measured albedo (the quotient of K↑ and K↓). Assuming that clear sky winter conditions at the Toronto, Ontario measurement site are typically associated with an influx of relatively non-turbid Arctic air, the atmospheric turbidity was initially fixed at an arbitrarily low value and adjusted slightly as required, to keep the error in the calculated value of the normal incidence direct beam irradiance within four percent, based on the assumption that the only source of error in the calculation of atmospheric attenuation lies in the specification of aerosol transmittance.

The results of the experiment are shown in figure 3.

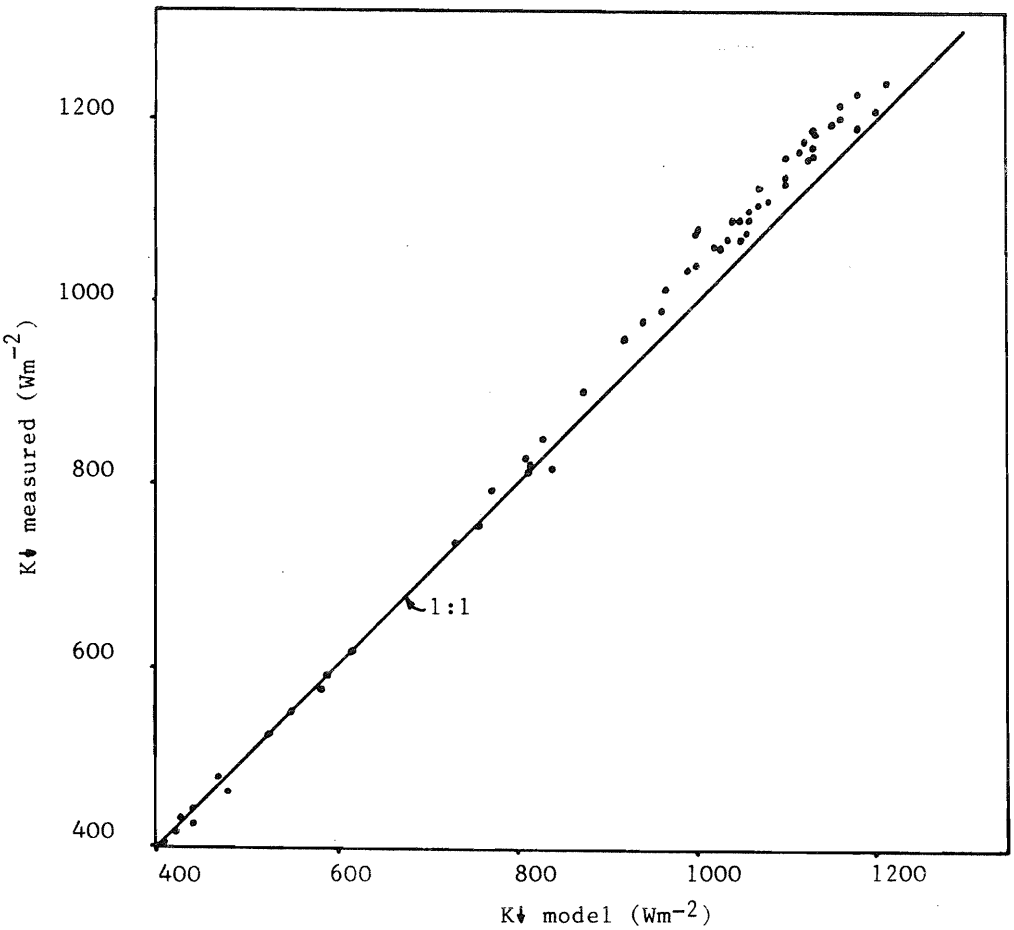

Figure 3. Comparison of the calculated and measured values of K↓ for the Toronto site.

For all radiometer orientations the root mean square error in the estimation of K↓ is less than the measurement error (estimated by Latimer (1972) to be five percent), ranging from ± 1.59 percent for the horizontal sensor to ± 4.52 percent for the vertical sensor. Nonetheless, the calculated data show a systematic underestimation of the total irradiance at increasing slope angles. Further examination of the data suggests that the source of this error lies in the calculation of the diffuse component of the total irradiance. The error is most probably due to two factors not accounted for by the model. The first is the brightening of the sky near the horizon. Although this effect can be incorporated into a solar radiation model by means of an empirical correction factor, as suggested by Temps and Coulson (1977), no effort has been made to include such a factor in the present model in order to facilitate its eventual application to areas of high relief where the distant horizon may be obscured. The second factor is the anisotropy of surface reflection, which

can be extremely high for some snow surfaces, as demonstrated by Middleton and Mungall (1952) and Christie (1953), among others. They demonstrate that the reflection pattern of many snow surfaces is characterized by a strong maximum in the forward direction (i.e. the azimuth of the incident radiation). Thus, the assumption that the reflected radiation is isotropically distributed may cause the model to underestimate the reflected component of the diffuse irradiance received by surfaces inclined toward the sun.

In view of the approximative nature of the atmospheric data input to the model, as well as the unknown characteristics of the surface surrounding the sensors, the errors in the model estimates of the incoming flux are acceptable. Given the direct relationship between the error in the flux calculations and the inclination of the sensor, the model should prove adequate for the less extreme slope angles typical of natural terrain. Indeed, the results of this and other experiments (Waterman, 1980a) suggest that the model is capable of reasonably accurate estimates of the instantaneous direct and diffuse shortwave irradiance incident upon inclined surfaces of any orientation in clear sky conditions, given average values of the atmospheric input parameters and a knowledge of the reflectance and irradiance characteristics of nearby terrain surfaces.

TOPOGRAPHIC EFFECTS

The dominant factor affecting the solar radiation received by a surface for given atmospheric and astronomic conditions is the angle of incidence of the solar beam, i, as shown in equation 2. However at a given wavelength, highly reflective terrain can alter this simple geometric relationship through atmospheric backscattering and terrain reflection, represented respectively by the $D\downarrow b$ and $D\downarrow r$ components of the incoming flux. In order to illustrate this problem, the model has been used to simulate the wavelength - integrated solar flux incident on a hypothetical array of radiometers suspended over a horizontal surface, inclined at various angles from the horizontal, and oriented in various azimuth directions relative to the sun. The atmospheric boundary conditions are those of a relatively non-turbid, dry air mass for an elevation of 3000 m ASL. These conditions minimize both the net attenuation of the solar flux by scattering processes and the anisotropy of the diffuse flux component. The solar zenith angle is fixed at 47.9 degrees (March 1, solar noon, 40 degrees N latitude). Values of $K\downarrow$ and $D\downarrow$ integrated between 0.285 and 2.8 μm were calculated for sensor inclinations in 10 degree intervals between horizontal and vertical positions, for azimuths relative to the sun of 0, 60, 120, and 180 degrees. The horizontal surface is assumed to be: a) non-reflecting, or b) a snow surface of spectral reflectance described by curve 1 in figure 2. The results of the calculations are shown in figures 4 and 5.

The results for a non-reflecting background show the combined effects of the cos i factor, which controls $S\downarrow$ and $D\downarrow cs$, and the $\cos^2(\gamma/2)$ factor, which affects both $D\downarrow i$ and $D\downarrow b$. The difference between $D\downarrow$ and $K\downarrow$ at a given azimuth for reflecting and non-reflecting backgrounds demonstrates the importance of the backscattered upwelling radiation, $D\downarrow b$, and the radiation reflected to the receiving surface from the adjacent horizontal surface, $D\downarrow r$. The backscattered flux is a maximum for a horizontal receiving surface, and decreases with increasing inclination of the surface. The maximum contribution of $D\downarrow b$ in this case is 36.9 Wm^{-2}, or 41.3 percent of the total diffuse flux incident on a horizontal surface. This represents a 70.4 percent increase in the total diffuse flux from the calculated value for the non-reflecting surface.

Despite the low scattering attenuation in this instance, the diffuse flux is slightly anisotropic, characterized by higher values of $D\downarrow$ for sunward facing (azimuth 0 degrees) surfaces. However, examination of figure 5 shows this effect to be less important in some topographic situations than the contribution of $D\downarrow r$ to the total diffuse flux. The calculated value of $D\downarrow$ for a vertical sunward facing sensor is 347.5 Wm^{-2} when the sensor faces a horizontal snow surface, but drops to 35.6 Wm^{-2} in the absence of surface reflection effects. The difference of 311.9 Wm^{-2} represents a backscattered flux of approximately 18.5 Wm^{-2} and 293.4 Wm^{-2} reflected to the receiving surface from the horizontal snow surface. For a sunward facing slope of 30 degrees, more typical of natural topography, $D\downarrow b$ and $D\downarrow r$ are more nearly equal, attaining values of 35.6 Wm^{-2} and 38.1 Wm^{-2}, respectively.

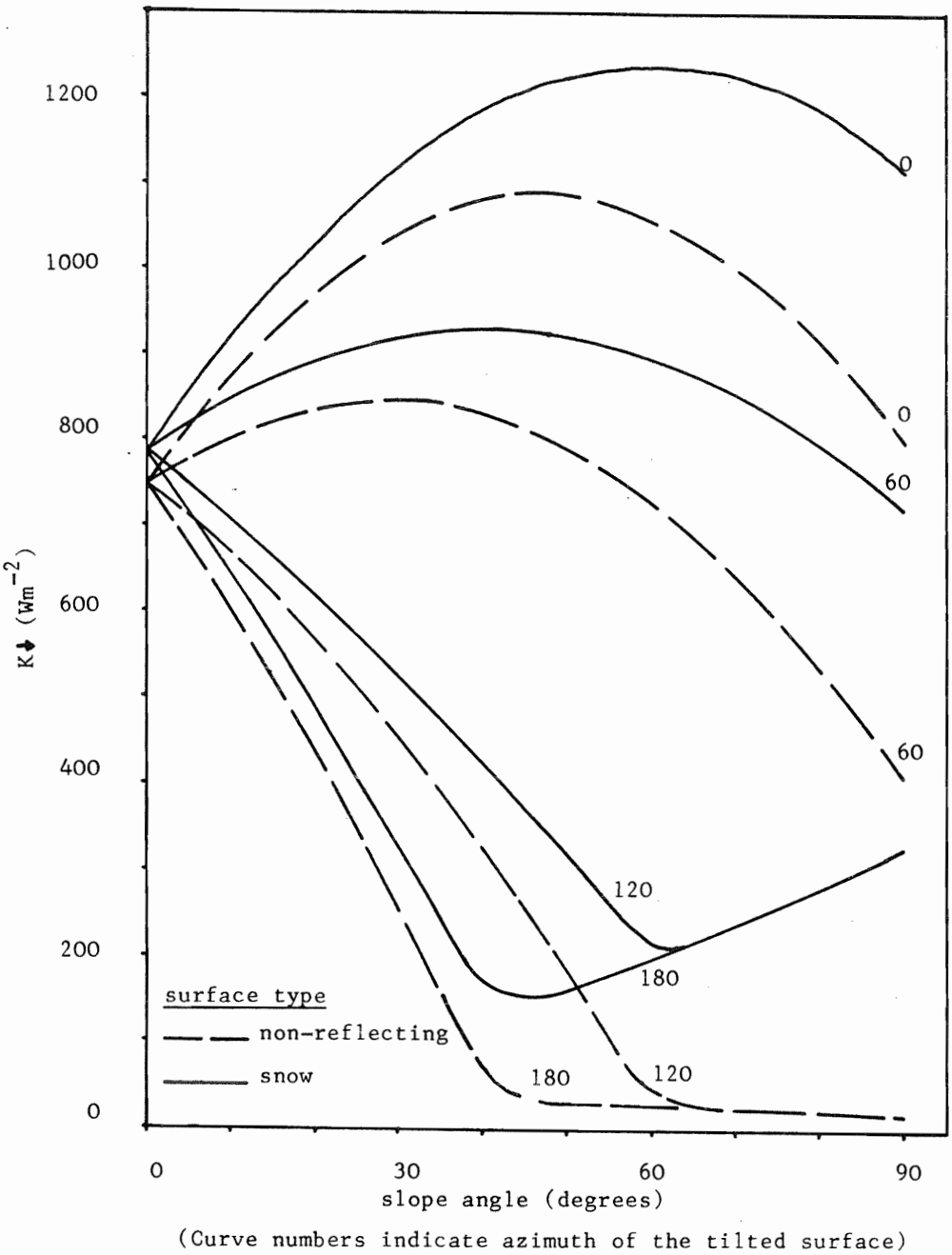

(Curve numbers indicate azimuth of the tilted surface)

Figure 4. Total irradiance received by inclined radiometers of varying orientation.

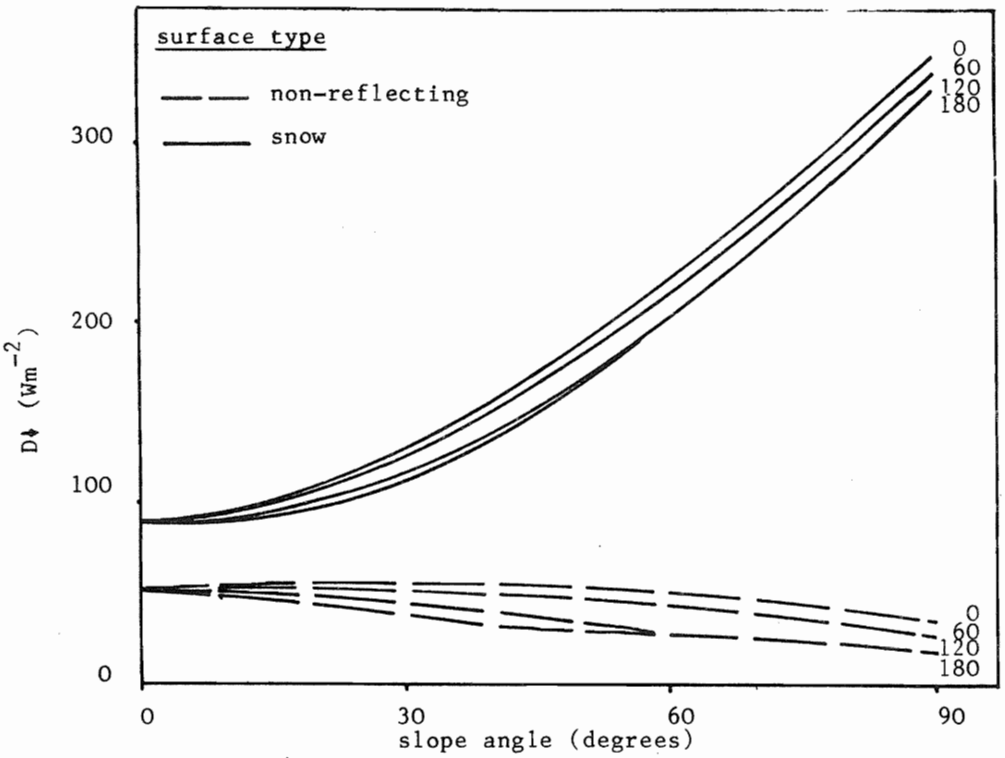

(Curve numbers indicate azimuth of the tilted surface)

Figure 5. Diffuse component of the total irradiance received by the inclined radiometers.

The results of this experiment show the way in which the presence of snow cover can affect the total incident irradiance. However, assessment of the impact of topographic effects on the net solar radiation further requires evaluation of the spectral characteristics of the incoming flux and the spectral reflectance properties of the surface in question. The direct and diffuse components of the total spectral irradiance incident on the horizontal snow surface in the preceding experiment are shown in figure 6. The bias of the diffuse irradiance to the shorter wavelengths, caused by the inverse wavelength dependence of both molecular and aerosol scattering, is clearly evident. The spectral distribution of the reflected solar flux, given the spectral reflectance characteristics of the snow surface described in figure 2 and the irradiance spectrum shown in figure 6, is shown in figure 7. This graph clearly shows that most of the solar radiation absorbed by the snow surface is in the near infrared region of the spectrum, as suggested by Choudhury and Kukla (1980). Comparison of figures 6 and 7 further shows that the direct component of the total irradiance provides virtually all of the radiation reaching the snow surface at those wavelengths where significant absorption occurs. The effect of topography on the net solar flux is thus seen to depend primarily upon the relationship between the terrain configuration and the near infrared irradiance.

A subset of the data presented in figures 4 and 5 can be used to demonstrate topographic effects on net solar radiation. In this case it is necessary to assume that the inclined radiometer is equivalent to a straight snow covered slope. This assumption is a reasonable one if the slope angle is such that the slope does not cast a shadow on the adjacent horizontal surface (Waterman, 1980a). This requirement is satisfied in this instance by restricting the calculations to slope angles of 40 degrees or less, a realistic range of slopes for mountainous terrain, although slopes of 40 degrees are unlikely to retain a significant depth of snow cover. The spectral reflectance characteristics of both the inclined receiving surface and the opposing horizontal surface are defined by curve 1 in figure 2. The results of the calculations for slopes oriented at 0 and 180 degrees relative to the sun are shown in Tables 1 and 2, respectively.

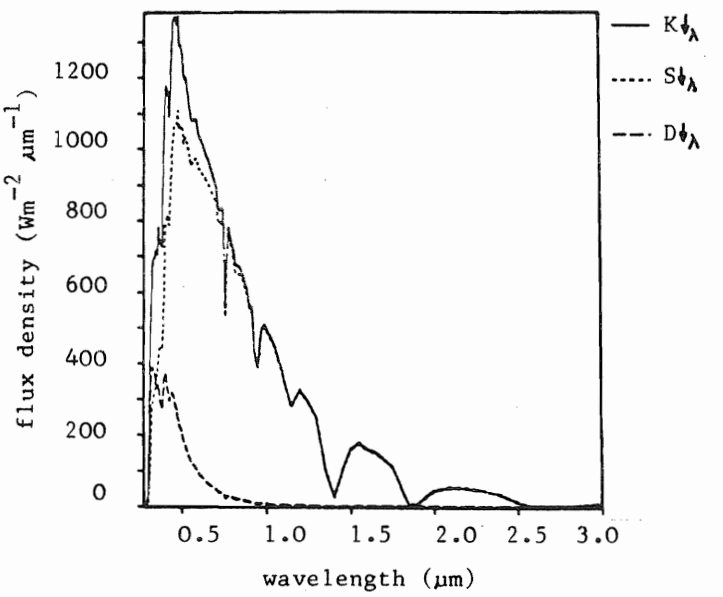

Figure 6. Spectral irradiance received by a horizontal snow surface.

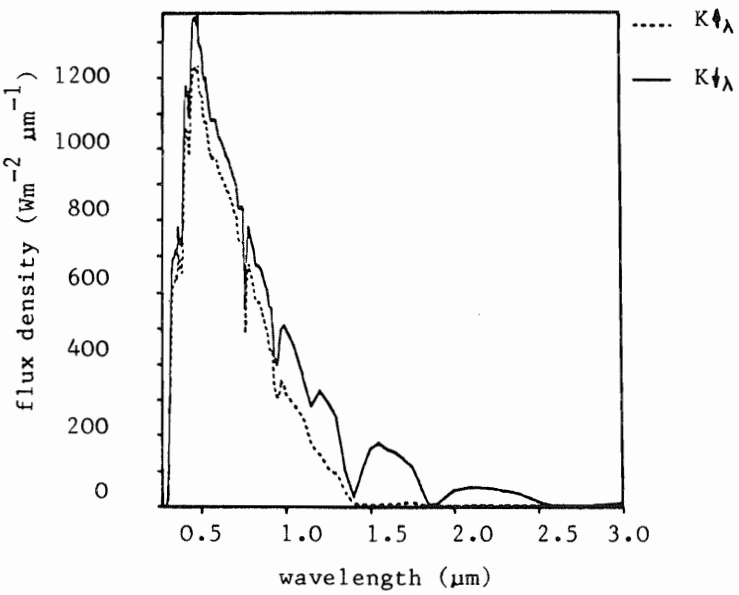

Figure 7. Spectral distribution of $K\downarrow$ and $K\downarrow$ for a horizontal snow surface.

Table 1. Components of the shortwave balance for an azimuth of 0°

a) horizontal surface is non-reflecting

	slope angle				
	0	10	20	30	40
K↓	748.0	873.6	973.3	1043.8	1083.3
K↑	550.9	642.4	714.9	766.1	794.6
K*	197.1	231.2	258.4	277.7	288.7
A	73.6	73.5	73.5	73.4	73.3

b) horizontal surface is snow covered

	slope angle				
	0	10	20	30	40
K↓	784.9	914.7	1026.7	1117.6	1184.5
K↑	583.9	678.9	761.8	829.9	881.3
K*	201.0	235.8	264.9	287.7	303.2
A	74.4	74.2	74.2	74.3	74.4

Table 2. Components of the shortwave balance for an azimuth of 180°

a) horizontal surface is non-reflecting

	slope angle				
	0	10	20	30	40
K↓	748.0	600.3	434.8	256.7	71.4
K↑	550.9	443.2	322.4	192.4	57.1
K*	197.1	157.1	112.4	64.3	14.3
A	73.6	73.8	74.1	75.0	80.0

b) horizontal surface is snow covered

	slope angle				
	0	10	20	30	40
K↓	784.9	641.4	488.3	330.5	172.6
K↑	583.9	479.7	369.3	256.2	143.8
K*	201.0	161.7	119.0	74.3	28.8
A	74.4	74.8	75.6	77.5	83.3

The complex interplay between the various components of the irradiance causes changes in the spectral distribution of the solar radiation incident on the snow surface, which are ultimately revealed in Tables 1 and 2 as variations in the albedo, A. When the terrain surrounding the slope is non-reflecting (Tables 1a and 2a), both $D\downarrow b$ and $D\downarrow r$ are zero, and changes in the albedo of the snow covered slope are due to the effect of changes in the angle of incidence of the direct solar beam on the spectral composition of the incoming radiation. This causes both $K\downarrow$ and K* to increase with increasing slope angle for the sunward facing slope (Table 1a), as a consequence of the increasing value of cos i, and the resultant increase in the effective contribution of both $S\downarrow$ and $D\downarrow cs$. This effect is accompanied by a reduction in the isotropically distributed diffuse flux caused by the $\cos^2(\gamma/2)$ factor. Because the direct solar beam and the circumsolar diffuse flux are the largest sources of near infrared radiation in this instance, and because the isotropic diffuse flux is concentrated in the shorter wavelengths where the spectral reflectance of the snow surface is low, the effective albedo of the snow surface decreases slightly as the slope increases. This trend is reversed for slopes facing away from the sun, as shown in Table 2a. In this case, the cos i factor causes the magnitude of $S\downarrow$ and $D\downarrow cs$ to decrease with increasing slope, leading to a shift in the irradiance spectrum to shorter wavelengths and a resultant increase in the albedo. Because the direct solar beam is the largest component of the incoming radiation, especially at near infrared wavelengths, as shown in figure 7, these effects lead to a rapid decrease in both $K\downarrow$ and K* with increasing incidence angle.

When the terrain surrounding the surface is also snow covered (Tables 1b and 2b), the incidence angle effect is modified by backscattered radiation, and radiation reflected to the slope from the adjacent horizontal surface. Since both of these flux components are assumed to be isotropic, their contribution to the total irradiance is independent of the azimuth of the slope. Because both $D\downarrow b$ and $D\downarrow r$ are concentrated in the visible wavelengths, as a consequence of molecular scattering and the spectral reflectance of snow, respectively, these components of the irradiance increase the effective albedo of the snow surface. In the case of a horizontal snow surface surrounded by snow covered terrain, backscattered radiation raises the total irradiance by 36.9 Wm^{-2} (4.9 percent), but the increase in K* is only 3.9 Wm^{-2} (2.0 percent), as a result of the spectral distribution of $D\downarrow b$. As a result, the albedo of the snow surface increases from 73.6 percent to 74.4 percent. As the slope of the surface increases, the contribution of $D\downarrow r$ increases with the factor $1 - \cos^2(\gamma/2)$, while $D\downarrow b$ decreases as $\cos^2(\gamma/2)$ decreases. If the slope faces the sun (Table 1b), the increase in the short wavelength diffuse flux is largely counterbalanced by the increase in $S\downarrow$ and $D\downarrow cs$, with the result that as the slope increases the albedo first decreases and then increases. At all slope angles, the albedo of the slope is greater if the horizontal surface is also snow covered. Consequently, although the total irradiance on the 40 degree slope increases 9.3 percent if both surfaces are snow covered, the increase in the net radiation is only 5.0 percent.

The contribution of the backscattered flux and terrain reflection is more significant when the angle of incidence of the direct solar beam is large, as shown in Table 2b. In this case, the addition of the $D\downarrow b$ and $D\downarrow r$ components increases the total irradiance incident on the 40 degree slope by approximately 142 percent. Primarily because a small amount of near infrared radiation is reflected from the horizontal surface, the net radiation increases by approximately 101 percent, while the albedo increases only slightly, from 80.0 percent to 83.3 percent.

DISCUSSION

The simple experiment described in the preceding section demonstrates that the interaction between the terrain and the shortwave radiation balance through the backscattering of upwelling radiation and the reflection of radiation from one surface to another is significant in areas of extensive snow cover. These factors are sufficient to double the net radiation available on a 40 degree slope oriented at 180 degrees relative to the sun, despite the relatively low near infrared reflectance of snow and the reduction in atmospheric backscattering at near infrared wavelengths. Both processes would be more significant if the surrounding terrain were more reflective in the near infrared. Terrain reflection takes on further significance for a shadowed surface (Waterman, 1980a,b), in which case both $S\downarrow$ and $D\downarrow cs$ are equal to zero, and $D\downarrow r$ is often the largest source of

near infrared radiation. Solar radiation models which fail to account for these factors are unlikely to be satisfactory for snow covered terrain.

The experiment results suggest that spectral flux models offer significant advantages over the wavelength - integrated models usually used in radiation balance calculations. A spectral flux model facilitates calculations of the backscattered diffuse flux and the anisotropy of the downward scattered radiation. Although these factors may be incorporated into wavelength - integrated models (Temps and Coulson, 1977, Hay, 1978b), the results are less satisfactory for snow covered terrain (Waterman, 1980a). Similarly, a spectral model offers advantages in calculations of radiation reflected to a point from other surfaces.

The preceding experiment demonstrates that the usual procedure of characterizing an inclined surface by an albedo measured for a horizontal surface is inadequate, because of changes in the spectral irradiance caused by the angle of incidence of the direct solar beam and/or topographic effects. In essence, the effective albedo of a snow surface is a function of the surrounding topography.

The importance of the near infrared irradiance in calculations of the net solar energy input to a snow surface, demonstrated in this study and by Dozier (1978) and Choudhury and Kukla (1980), coupled with the low intensity of $D\downarrow b$ and $D\downarrow i$ in the near infrared, leads to pronounced topographic control of the net solar radiation in snow covered terrain, primarily through the changing incidence angle of the direct solar beam. The importance of the direct beam irradiance suggests that the diffuse flux may be disregarded in some instances. This approach may be adequate, for example, in studies where net solar radiation data are required for calculations of snowmelt over a large area, because the solar radiation available for snowmelt on sunlit surfaces is far greater than the energy available on shadowed surfaces. This procedure would significantly reduce the complexity of the model. However, the results of this study suggest that detailed spectral evaluation of all aspects of the shortwave radiation balance, including backscattering and terrain reflection, is required for smaller scale investigations.

REFERENCES

Angstrom, A., 1961: Techniques for determining the turbidity of the atmosphere. Tellus 13, 214-223.

_____, 1964: The parameters of atmospheric turbidity. Tellus 16, 64-75.

Choudhury, B., and G. Kukla, 1980: Impact of CO_2 on cooling of snow and water surfaces. Nature 280, 668-671.

Christie, A.W., 1953: The luminous directional reflectance of snow. Jour. Opt. Soc. Am. 41, 621-622.

Dozier, J., 1978: A solar radiation model for a snow surface in mountainous terrain. 144-153 in Colbeck, S.C. and M. Ray (eds.), Modeling Snow Cover Runoff, U.S. Army Cold Regions Research and Engineering, Hanover, N.H., Sept. 25-29, 1978.

Garnier, B.J., and A. Ohmura, 1978: A method of calculating the direct shortwave income of slopes. Jour. Appl. Meteor. 7, 796-800.

_____, 1970: The evaluation of surface variations in solar radiation income. Solar Energy 13, 21-34.

Hay, J.E., 1978a: Measuring and modelling of shortwave radiation on inclined surfaces. Proc. Third Conference on Atmospheric Radiation. June 28-30, 1978, Davis, California.

_____, 1978b: An Analysis of Solar Radiation Data for Selected Locations in Canada. Climatological Studies No. 32, Atmospheric Environment Service, Toronto, 158 pp.

Houghton, H.B., 1954: On the annual heat balance of the northern hemisphere. Jour. Meteor., 11, 1-9.

Leckner, B., 1978: The spectral distribution of solar radiation at the earth's surface - elements of a model. Solar Energy, 20, 143-150.

Middleton, W.E., and A.G. Mungall, 1952: The luminous directional reflectance of snow. Jour. Opt. Soc. Am., 42, 572-579.

Obled, C., and H. Harder, 1978: A review of snow melt in the mountain environment. 179-204 in Colbeck, S.C. and M. Ray (eds.), Modeling Snow Cover Runoff, U.S. Army Cold Regions Research and Engineering Laboratory, Hanover, N.H., 25-29 Sept., 1978.

O'Brien, H.W., and R.H. Munis, 1975: Red and Near-Infrared Reflectance of Snow. U.S. Army Cold Regions Research and Engineering Laboratory, Res. Rept. 332, 18 pp.

Paltridge, G.W., and C.M.R. Platt, 1976: Radiative Processes in Meteorology and Climatology. Wiley and Sons, New York.

Robinson, N. ed., 1969: Solar Radiation. Elsevier Publishing Co., Amsterdam, 347 pp.

Temps, R.C., and K.L. Coulson, 1977: Solar radiation incident upon slopes of different orientations. Solar Energy, 19, 179-184.

Thekaekara, M.P., 1973: Solar energy outside the earth's atmosphere. Solar Energy, 14, 109-127.

Waterman, S.E., 1980a: Investigation of multispectral remote sensing of snow cover using a solar radiation model. Unpub. Ph.D. Thesis, University of Colorado.

_____, 1980b: Investigation of multispectral remote sensing of snow cover using a solar radiation model. Proceedings of the 6th Canadian Symposium on Remote Sensing, Halifax, N.S., May 1980 (in press).

Williams, L.D., R.G. Barry, and J.T. Andrews, 1972: Application of computed global radiation for areas of high relief. Jour. Appl. Meteor., 11, 526-532.

LIST OF SYMBOLS

A	Albedo
$D\downarrow_\lambda$	Diffuse spectral irradiance
$D\downarrow b_\lambda$	Backscattered diffuse spectral irradiance
$D\downarrow cs_\lambda$	Circumsolar diffuse radiation
$D\downarrow i_\lambda$	Isotropic diffuse radiation
$D\downarrow r_\lambda$	Diffuse radiation reflected from one terrain surface to another
$D\downarrow s_\lambda$	Scattered downwelling radiation
Df_λ	Downward scattered radiation
f_λ	Forward scattering factor
fi_λ	Isotropic scattering factor
i	Incidence angle of the solar beam
I_λ	Normal incidence direct irradiance
$I_{o\lambda}$	Extraterrestrial irradiance
ΔIs_λ	Total scattered radiation
$K\downarrow_\lambda$	Spectral irradiance
$K\uparrow_\lambda$	Reflected spectral flux
K^*_λ	Net monochromatic radiation
p_λ	Spectral reflectance
pa_λ	Effective spectral reflectance of the atmosphere
ps_λ	Spectral reflectance of the background surface
r	Radius vector of the earth's orbit
$S\downarrow_\lambda$	Direct beam irradiance

Ta_λ	Aerosol scattering spectral transmittance
Tg_λ	Spectral transmittance of mixed gases
Toz_λ	Spectral transmittance of ozone
Tr_λ	Rayleigh scattering spectral transmittance
Tw_λ	Spectral transmittance of water vapour
z	Zenith angle of the sun
λ	Wavelength (um)
γ	Slope angle